

# Caloric Curves and Critical Behavior in Nuclei

J. B. Natowitz, R. Wada, K. Hagel, T. Keutgen, M. Murray, A. Makeev, L. Qin, P. Smith, and C. Hamilton  
*Cyclotron Institute, Texas A&M University,*  
*College Station, Texas, 77845*  
 (Dated: October 29, 2018)

Data from a number of different experimental measurements have been used to construct caloric curves for five different regions of nuclear mass. These curves are qualitatively similar and exhibit plateaus at the higher excitation energies. The limiting temperatures represented by the plateaus decrease with increasing nuclear mass and are in very good agreement with results of recent calculations employing either a chiral symmetry model or the Gogny interaction. This agreement strongly favors a soft equation of state. Evidence is presented which suggests that critical excitation energies and critical temperatures might be determined from caloric curve measurements when the mass variations inherent in such measurements are taken into account.

PACS numbers: 24.10.i,25.70.Gh

## I. INTRODUCTION

Measurements of the nuclear specific heat have long been considered to be a technique that should provide important information on the properties of excited nuclei and the postulated liquid-gas phase transition [1, 2, 3, 4, 5]. Over slightly more than a decade a number of measurements have been motivated by this expectation [6, 7, 8, 9, 10, 11, 12, 13, 14, 15, 16, 17, 18, 19]. However, given the significant variation in the systems studied, in the collision dynamics involved, in the experimental and analysis techniques employed, in the theoretical descriptions proposed and even in the way the results are reported, a coherent picture of the information content in caloric curves has been difficult to obtain. Indeed, two recent reviews of caloric curve measurements [20, 21] have reached rather pessimistic conclusions on the utility of such measurements. We present evidence that, in fact, the existing body of data provides a rather consistent picture when the mass dependence of the caloric curve measurements is taken into account. Further, comparison with the results of a recently reported Fisher Droplet Model analysis establishing the critical point in the  $A \sim 160$  region [22] indicates that the available caloric curve data provide direct measures of both the critical energy and the critical temperature for the phase change into a *non-monomeric* gaseous phase over a wide range of nuclear masses.

## II. ANALYSIS AND RESULTS

### A. Selection of Data

We present in this paper an analysis of the combined results of temperatures and excitation energies of references [6, 7, 8, 9, 10, 11, 12, 13, 14, 15, 16, 17, 18, 19]. We have selected these results because in each of the cases considered the authors have attempted a simultaneous derivation of the *initial* temperatures of de-exciting nuclei of reasonably well characterized nuclear masses and

excitation energies. Except at the lowest projectile energies, a de-convolution of product energy and yield spectra is usually required in order that these properties may be established. Typically, phenomenological or theoretical corrections must be applied to measured values to obtain the desired initial values. This is usually necessary in the case of the measured *apparent* temperatures, whether slope temperatures [6, 7, 8, 9, 10] or double isotope yield ratio temperatures [11, 12, 13, 14, 15, 16, 17, 18, 19, 23], to account for de-excitation cascades and secondary particle contributions.

To obtain the initial thermal excitation energies, corrections for unobserved ejectiles, i.e. neutrons, gamma rays (small and sometimes neglected) and undetected charged species are often needed. In one case, statistical model calculations have been employed to “back-trace” the excitation energy [12]. Where corrections to the raw observed values are required, they have been applied in the referenced works or sufficient information has been given to allow such corrections to be made for the present analysis. In Table 1 the experimental investigations which are the sources of the data included in our analysis are listed together with an indication of the techniques used to extract and to correct the excitation energies and temperatures. Much more detail on the methods employed to analyze the experiments and to make the corrections required to determine the excitation energies and temperatures of the primary hot composite nuclei is presented in the references [6, 7, 8, 9, 10, 11, 12, 13, 14, 15, 16, 17, 18, 19]. Below we make only a few additional comments on some of these papers to better explain our use of the available information found there. We emphasize that the goal in each case is to determine the excitation energy and temperature of the primary composite system that remains after early non-equilibrium emission processes subside.

1. The Aladin Collaboration has determined temperatures by multiplying observed double isotope,  $T_{HeLi}$ , temperatures by a factor of 1.2 [11]. This factor, intended to correct the observed data for effects of secondary emission data, was determined from Quantum

Statistical Model calculations. While the initially reported caloric curve for this system relied on calorimetric techniques for energy determination, more recently, in reference [12], a back-tracing technique was employed to determine the thermal excitation energy after the early non-equilibrium emission phase of the reaction. This is done by requiring that the mass distributions and other observables, calculated using the SMM model, agree with the measured distributions. We utilize this more recent thermal energy determination and the caloric curve presented in Figure 61 of reference [12].

2. In reference [13], Hauger *et al.* present results for their analysis of the data for 1GeV/nucleon  $^{84}\text{Kr}$ ,  $^{139}\text{La}$  and  $^{197}\text{Au}$  beams on  $^{12}\text{C}$  targets. Initial Excitation energies and masses were obtained by subtracting the energy and mass removed in the pre-equilibrium stage of the reaction (see Figures 12 and 18 of Ref [13].) Initial temperatures were derived from the SMM model calculations which employed the experimental initial excitation energies and masses and were found to be in good agreement with the final observed distributions. Thus it is the “hot caloric curves” presented in Figure 20 of reference 13 which are used in this paper.

3. For the experiments of the ISiS collaboration [15, 16, 19] initial excitation energies and masses are also obtained by subtracting the energy and mass removed in the pre-equilibrium stage of the reaction. Raw temperatures are determined with a relatively high selection of ejectile energy range in the remaining spectrum. Some sensitivity to the selected range is observed. Since the pre-equilibrium component has been removed this sensitivity appears to be indicative of cooling in the investigated systems. In references [14, 15] which report measurements for  $^3\text{He}$  projectiles with  $^{197}\text{Au}$  and Ag, temperatures are not corrected for this effect. However, comparisons of the results of SMM calculations for the  $^3\text{He} + ^{197}\text{Au}$  system, with and without energy cuts equivalent to those used in the experiments, are presented. The comparison allows estimation of the factors required to correct the apparent temperatures. We have corrected the Ag data by assuming the same correction factors apply. In reference [19] the temperatures are corrected for secondary decay using parameters suggested by Tsang *et al.* [24]. These corrections are relatively small, typically less than 10%.

4. The temperatures of references [17, 18] are established for identical velocity species in a coalescence type of analysis. No temperature correction is applied as the techniques employed should be effective at discriminating against secondary decay contributions. Excitation energies are determined calorimetrically.

Only some of the experiments summarized in Table 1 have measured neutron multiplicities [10, 11, 12, 14, 17, 18] and only two have measured neutron spectra [10, 12]. The other experiments employing calorimetric techniques determine the neutron emission contribution to the thermal energy using phenomenological corrections based upon related observations and/or statistical

calculations. At low excitations where neutron emission dominates this can lead to larger uncertainties [25]. It may also lead to systematically larger uncertainties at the higher limits of the apparent excitation energy spectrum where fluctuations may be significant [26]. In general both excitation energies and temperatures appear to be subject to systematic uncertainties of  $\approx 10\%$  in the various experiments [26].

Additional information on caloric curves has been reported by the INDRA collaboration [27, 28, 29]. It is our understanding that the excitation energy determinations and temperatures for those experiments are currently under review [30] and therefore we have not included them in this work.

## B. Correlation of Temperature, Excitation Energy and Mass

In Fig. 1 we plot the correlated values of the temperatures and excitation energies per nucleon which have been determined in the experiments represented in Table 1. For comparison we plot curves corresponding to Fermi-gas model predictions with inverse level density parameters  $K=8$  and  $K=13$ . Also included for a further reference is a “total vaporization” line representing the (purely hypothetical) two-stage scenario of separation into constituent nucleons, at a cost of 8 MeV/nucleon followed by thermal heating. Although there is a significant increase in divergence of the results at higher excitation energies, the combined data still exhibit the qualitative features observed previously in many of the individual experiments, i.e. an apparent Fermi gas-like rise at excitation energies per nucleon below 3-4 MeV/nucleon, a very slow rate of temperature increase at higher energies ( $\sim 4-9$  MeV/nucleon) and some indication of an increase again at higher energy,  $\sim 9$  MeV/nucleon.

In some of the experiments considered the more central collisions were selected by an appropriate experimental filter and the excitation energy was varied by changing the projectile energy [9, 10, 17, 18]. In such cases the masses of the excited systems ( following pre-equilibrium emission) are reasonably well constrained. In other experiments a single projectile energy was used and a range of impact parameters from peripheral to central was investigated [6, 7, 8, 11, 12, 13, 14, 15, 16]. In those cases the initial masses, and excitation energies of the excited systems studied may vary significantly with impact parameter. That the results included in Fig. 1 include experiments which span a broad range of mass is illustrated in Figs. 2 and 3 which present plots of the primary excitation energies and temperatures as a function of the derived values of the primary mass. The wide mass variation inherent in many of the individual experiments is clear as is the fact that different experiments may sample the same mass range at significantly different excitation energies. We have previously suggested that mass variation is an important factor which should be considered

in any interpretation of the caloric curve [31].

### C. Caloric Curves for Restricted Mass regions

In order to explore the extent to which the variations in reported caloric curves seen in Fig. 1 are affected by mass variation we have constructed composite caloric curves for five different mass regions by combining the appropriate data from each of the systems of Table I. In Fig. 4 (a)-(e) we present the resultant curves for the mass number regions 30-60, 60-100,100-140,140-180 and 180-240. For comparison each sub-figure also includes the calculated Fermi gas curves for  $K=8$  and  $K=13$ , as well as the “total vaporization” line presented in Fig. 1.

Viewed in this way the resultant curves are qualitatively similar, in general rising at low energies, trending towards the  $K=13$  line, and then leveling into a plateau-like region. The quantitative aspects of the behavior in the lower energy region and the importance of the temperature dependence of the effective mass in determining the level density parameter have previously been extensively discussed [32, 33, 34]. The rise toward  $K=13$  and flattening of the curve, representing a sharp rise in the heat capacity, has been discussed [31, 35] and compared with model predictions. In statistical models of multifragmentation the break occurs at a “cracking energy” which represents the onset of multiple fragment production [3, 4]. Within the framework of classical molecular dynamics calculations [36, 37] quantum molecular dynamics calculations [38, 39] and more microscopic treatments [40, 41] plateaus are also observed.

For the lightest mass window,  $A=30-60$ , the increase above  $K=8$  is less pronounced but there is evidence of a flattening near 8 MeV/nucleon excitation energy. For the next three windows this feature appears near 4 MeV/nucleon excitation. For the highest window it seems to occur even lower, near 3 MeV/nucleon. Although there is considerable spread in the data, we have determined the average temperatures in the plateau regions for each mass window. This was done by using the data at excitation energies above the points where the flattening appears to set in. The results of temperature measurements for excitation energies  $> 9$  MeV/nucleon, noted above in the discussion of Fig. 1 as suggesting a later rise in the caloric curve, are seen in Fig. 4 to be dominated by the data in the lowest mass window,  $A=30-60$ , and the three highest excitation energy points from reference [19], which fall in the  $A=100-140$  mass window (Fig. 4 (c) ). In the  $A=30-60$  mass window the evidence for this later rise is now less compelling and the data have been used in determining the average. The three points at highest excitation in Fig. 4 (c) may signal a further rise and have not been included. For the data of reference [19], the reported uncertainties for the highest excitation energy points become larger than the nominal 10% systematic value which we have assumed for all points. The average values are shown as solid horizontal

lines in Fig. 4 (a)-(e). We note that the width of the selected mass windows still allows for some mass variation and individual experiments in which the mass is changing show some evidence of an increase in the more restricted mass windows. Nevertheless, the general agreement of the data with the average leads to relatively small standard deviations on these averages.

In Fig. 4 the value of the limiting temperature reached in the plateau decreases with increasing mass. It has previously been suggested [35, 36] that the limiting temperatures which are observed in Caloric curve measurements represent the “Coulomb instability” temperatures, first calculated with a temperature dependent Hartree-Fock model employing a Skyrme interaction [2, 42, 43] and later with other models [40, 44, 45, 46]. In such calculations, the limiting temperature, which represents the limit of equilibrium phase coexistence between liquid and vapor, has been designated as the point of Coulomb instability because, in the absence of the Coulomb forces the coexistence is possible up to the critical temperature of nuclear matter [2]. The observed Coulomb instability temperature has been related to the incompressibility and critical temperature of nuclear matter [43]. Limiting temperature data for  $A\sim 120$  from reference [7] were found to be in best agreement with results of those calculations when the SJ1 Skyrme interaction was used [31, 35].

As noted above, for nuclei with  $A > 60$ , the flattening of the caloric curve sets in at similar excitation energies. In Fig. 5, we use all data for  $A > 60$  to present another view of the evolution of the temperature-excitation energy correlations. Fig. 5 depicts the variation of the apparent inverse level density parameter with excitation energy, calculated assuming Fermi gas behavior,  $K = T^2/(E^*/A)$ . At low excitation energy the apparent inverse level density parameter increases from  $K=8$  to higher values as predicted in models which take into account the change in effective nucleon mass [32, 33, 34]. The solid line with solid points presented on the figure shows the results of one such calculation [33].

At higher excitation, however, there is a systematic change observed. At excitation energies in the 3-5 MeV/nucleon range the derived values of  $K$  start decreasing. Although there is some scatter in the experimental points, the overall dependence of  $K$  on excitation energy manifests the limiting temperature behavior seen in Fig. 4 and demonstrates quite clearly a qualitative change in the excited nuclei being investigated. With increasing excitation the values become progressively smaller. At the highest excitation energies they have fallen well below the value of 8 initially derived at low excitation.

For the highest excitation energy data of reference [19], the higher reported temperatures lead to significantly higher apparent  $K$  values. This is a potentially interesting behavior but is different than that derived from the other measurements which sample that excitation energy range. In reference [19], the reported uncertainties for those points are larger than the nominal 10% system-

atic value which we have assumed for all points. Also, the effect of energy cut and application of the Tsang systematics [24] in an excitation energy range well above that for which that systematics was established may be affecting these results.

### III. DISCUSSION & INTERPRETATION

#### A. Limiting temperatures and Coulomb Instabilities

As seen in the preceding section, while the curves for each mass region rise then flatten, the values of excitation energy and temperature at which this transition takes place appear to decrease with increasing mass. To further quantify this observation we have applied, for each mass region, a fit to the lower energy data to determine the point of transition from Fermi-gas-like behavior to the plateau region. For this purpose we used  $T = \sqrt{K(E^*/A)}$ . Recognizing the increase in  $K$  which occurs in that region, we have restricted the fits to the points near the transition. The results of these fits are shown in Fig. 4 (a)-(e). For the different mass windows, the derived limiting temperatures are plotted in Fig. 6(a) and the excitation energies at which these limits are reached are plotted in Fig. 6(b). The values of both  $T$  and  $E^*/A$  at the transition point drop significantly as the mass increases. For comparison with the derived limiting temperatures we also present Coulomb instability limiting temperatures calculated by Zhang et al. [46], employing both a relativistic chiral symmetry model [47] and the Gogny GD1 interaction [45]. For both, the calculated temperatures are in very close agreement with the average temperature values derived from the plateau regions of the caloric curves.

The good agreement between the experimental points and the values calculated using either the chiral symmetry model (designated FST model in reference [46]) or the Gogny interaction favors a soft equation of state. The nuclear matter incompressibility in the FST model with the T1 parameterization is 194 MeV. For the Gogny GD1 interaction it is 228 MeV. Thus the experimental results of this analysis are in accord with the incompressibilities derived from Giant Monopole Resonance data [48]. For finite symmetric nuclear matter the temperature dependence of the surface energy is taken to be that suggested by Goodman et al. [49]. The critical temperature of the FST model with the T1 parameter set is 14.8 MeV. It is 15.9 MeV when the Gogny GD1 force is employed.

#### B. Critical Points in Nuclei

The question of the significance of the transition points presented in Fig. 5 may additionally be addressed using recently reported results of a Fisher Droplet Model analysis. The use of the Fisher droplet analysis to isolate pos-

sible critical behavior in nuclei has been extensively explored by the EOS collaboration [50] and critical parameters of the model have been extracted. Recently, Elliott *et al.* [22] have carried out a Fisher Droplet Model analysis of the high-statistics multifragmentation data of the ISiS collaboration for 8 GeV/c pions on  $^{197}\text{Au}$  [19] and shown that an impressive universal scaling of the data is achieved up to an excitation energy of 3.8 MeV/nucleon at which point the scaling is lost. This scaling behavior is found to be identical to that observed in three dimensional Ising model calculations which model liquid-vapor co-existence [22, 51]. The scaled data are interpreted as defining the liquid-gas co-existence line and the excitation energy of 3.8 MeV is identified as the critical energy for the system under investigation.

By assuming Fermi gas behavior up to the critical point, and an inverse level density parameter of  $K=13$ , Elliott *et al.*, [22] conclude that the critical temperature is 6.7 MeV. (In reference [19] the corrected double isotope ratio temperatures at 3.8 MeV/nucleon excitation are 6.5 MeV.) In the experiment the excitation energy of 3.8 MeV/nucleon is associated with masses near  $A\sim 168$  (see Fig. 4 (d)). Inspection of the  $\pi + ^{197}\text{Au}$  caloric curve in Fig. 1 shows that  $E^*/A = 3.8$  MeV and  $T = 6.7$  MeV is essentially the point at which that caloric curve departs from Fermi gas-like behavior. *Thus this point of flattening and rapid departure of the caloric curve from the Fermi-gas like behavior is the point identified as the critical point by the droplet analysis.*

Clearly, it would be very interesting to have data of sufficient statistics to carry out Fisher droplet model analyses in the different mass regions for which caloric curves have been determined. However, given that the critical point identified by the droplet analysis is the point of the observed departure from the Fermi gas behavior and flattening of the caloric curve, the equivalent points in other mass regions may define the critical energies and temperatures for those mass regions.

The critical excitation energy and temperature determined from the droplet analysis of the ISiS data are plotted in Fig. 6. There it can be seen that the critical point determined in the droplet analysis is slightly higher than the transition point derived from the ensemble of caloric curve data in the 140-180 mass region. This is a direct reflection of the fact that the deviation of the ISiS results from the Fermi gas-like behavior occurs at higher excitation and temperature than indicated by the totality of experiments providing information in this mass region, see Fig. 4(d). Similarly, our recently published results for collisions at 47MeV/A projectile energy [17, 18] indicate, for the  $A=100-140$  region, a slightly higher critical excitation energy and critical temperature than is obtained from the totality of the data in that mass region. Such comparisons with selected experiments emphasize the importance of accurate determinations of both  $E^*/A$  and  $T$  to the quantitative establishment of the critical points.

#### IV. SUMMARY AND CONCLUSIONS

Data from a number of different experimental measurements have been combined to construct caloric curves for five regions of nuclear mass. These curves are qualitatively similar and exhibit plateaus at higher excitation energies. For the  $A \sim 160$  region, the critical point identified by a recent Fisher droplet model analysis [22] is observed to coincide with the point of the observed departure from Fermi gas-like behavior and flattening in the caloric curve. This information is used to derive possible critical points from the caloric curves for other mass regions. These temperatures and excitation energies are seen to decrease with increasing nuclear mass. The values are in very good agreement with results of recent calculations employing either a relativistic mean field treatment or the Gogny interaction. This agreement favors a soft equation of state with an incompressibility of 194-228 MeV and a critical temperature of 14.8-15.9 MeV for symmetric nuclear matter. It should be noted, however, that the calculations are made for beta stable nuclei while the experiments tend to produce nuclei somewhat away from beta stability, on either side depending upon the system studied and the first stage reaction dynamics. The fluctuations which this might cause in the experimental results are comparable to the assumed systematic uncertainties in the measurements [44, 52].

The combined observations suggest near achievement of liquid-gas equilibrium analogous to that assumed in the Coulomb instability calculations. Reaching such a condition in these rapidly evolving systems may require that the collision dynamics leads to a rapid filling of the available phase space-as suggested in recent discussions of apparent chemical equilibrium in experiments looking for the “other” phase change at relativistic energies [53].

As indicated, it would be very interesting to have data of sufficient statistics to carry out Fisher droplet model analyses in the different mass regions for which caloric curves have been determined. Still it is worth noting that, while Fisher Droplet analyses may provide the essential demonstration of critical behavior, a precise identification of the excitation energy and temperature at the critical point will continue to rely on measurements of the

type surveyed here.

Extension of such measurements to nuclei with very different  $N/Z$  ratios would also be very interesting. Significant differences in limiting temperatures should be seen in more asymmetric systems and the order of the phase transition is expected to change [44, 52, 54]. For the systems already studied, the differences in the entrance channel isospins and in the first stage dynamics lead to some variation of the isospin of the fragmenting nuclei. However the systematic uncertainties in the present measurements are such that sensitivity to this variable is not obvious. With radioactive beams it should be possible to employ caloric curve measurements to determine the critical parameters for quite asymmetric nuclei, thus testing the isospin dependence of the equation of state. For such beams, the intensity limitations far from stability will mean that caloric curve measurements will be inherently easier to obtain than will the high statistics data needed for a droplet analysis. Caloric curve measurements should continue to be an important tool for probing the equation of state.

Note added: Following submission of this paper, Srivastava *et al.* [55] have submitted a preprint reporting results of a systematic analysis of the moments of the fragment size distributions in their EOS data. This analysis also indicates a decrease in temperature and excitation energy with increasing mass, which they attribute to Coulomb effects. Also, Dorso and Bonasera [56] have recently published results of an analysis of molecular dynamics calculations which identified the region of entry into the plateau as the region where fluctuations are maximal and critical behavior could be expected.

#### V. ACKNOWLEDGEMENTS

We thank W. Trautmann, D. Cussol, A. Ruangma, A. Hauger and B. Srivastava for providing us with numerical values of their data. We appreciate very useful conversations with Shalom Shlomo and H. Q. Song. This work was supported by the U S Department of energy under Grant DE-FG03-93ER40773 and by the Robert A. Welch Foundation.

- 
- [1] E. Suraud, C. Gregoire and B. Tamain, Prog. Part. and Nucl. Phys. **23**, 357 (1989) and references therein.
  - [2] P. Bonche, S. Levit and H. Vautherin, Nucl. Phys. **A427**, 278 (1984); *Ibid*, **A436**, 265 (1986).
  - [3] D. Gross et. al. Prog. Part. and Nucl. Phys. **30**, 155 (1993) and references therein.
  - [4] J. Bondorf et al., Nucl. Phys. **A433**, 321 (1985).
  - [5] W. A. Friedman Phys. Rev. Lett. **60**, 2125 (1988).
  - [6] K. Hagel, D. Fabris, P. Gonthier, H. Ho, Y. Lou, Z. Majka, G. Mouchaty, M. N. Namboodiri, J. B. Natowitz, G. Nebbia, R. P. Schmitt, G. Viesti, R. Wada and B. Wilkins Nucl. Phys. **A486**, 429 (1988).
  - [7] R. Wada, D. Fabris, K. Hagel, G. Nebbia, Y. Lou, M. Gonnin, J. B. Natowitz, R. Billerey, B. Cheynis, A. Demeyer, D. Drain, D. Guinet, C. Pastor, L. Vagneron, K. Zaid, J. Alarja, A. Giorni, D. Heuer, C. Morand, B. Viano, C. Mazur, C. Ngo, S. Leray, R. Lucas, M. Ribrag and E. Tomasi, Phys. Rev. C **39**, 497 (1989).
  - [8] D. Cussol, G. Bizard, R. Brou, D. Durand, M. Louvel, J.P. Patry, J. Peter, R. Regimbart, J. C. Steckmeyer, J.P. Sullivan, B. Tamain, E. Crema, H. Doubre, K. Hagel, G.M. Jin, A. Peghaire, F. Saint Laurent, F. Cassagnou, R. Legrain, c. LeBrun, E. Rosato, R. Mac Grath, S. C. Jeong, S. M. Lee, Y. Nagashima, T. Nakagawa, M. Ogihara,

- J. Kasagi and T. Motobayashi, Nucl. Phys. **A561**, 298 (1993).
- [9] E. Chulick, unpublished data
- [10] M. Gonin et. al. Phys. Rev. C **42**, 2125 (1990).
- [11] J. Pochadzalla T. Mhlenkamp, T. Rubehn, A. Schttauf, A. Wrner, E. Zude1, M. Begemann-Blaich, Th. Blaich, H. Emling, A. Ferrero, C.Gross, G. Imm, I. Iori, G. J. Kunde, W. D. Kunze, V. Lindenstruth, U. Lynen, A. Moroni, W. F. J. Mller, B.Ocker, G. Raciti, H. Sann1, C. Schwarz, W. Seidel, V. Serfling, J. Stroth, W. Trautmann, A. Trzcinski, A. Tucholski, G. Verde, and B. Zwieglinski, Phys. Rev. Lett. **75**, 1040 (1995).
- [12] T. Odeh, GSI Report Diss. 99-15, August, 1999 and references therein.
- [13] J. A. Hauger, B. K. Srivastava, S. Albergo, F. Bieser, F. P. Brady, Z. Caccia, D. A. Cebra, A. D. Chacon, J. L. Chance, Y. Choi, S. Costa, J. B. Elliott, M. L. Gilkes, A. S. Hirsch, E. L. Hjort, A. Insolia, M. Justice, D. Keane, J. C. Kintner, V. Lindenstruth, M. A. Lisa, H. S. Matis, M. McMahan, C. McParland, W. F. J. Mueller, D. L. Olson, M. D. Partlan, N. T. Porile, R. Potenza, G. Rai, J. Rasmussen, H. G. Ritter, J. Romanski, J. L. Romero, G. V. Russo, H. Sann, R. P. Scharenberg, A. Scott, Y. Shao, T. J. M. Symons, M. Tincknell, C. Tuve, S. Wang, P. Warren, H. H. Wieman, T. Wienold, and K. Wolf, Phys. Rev. C **62**, 024616 (2000).
- [14] R. Wada, R. Tezkratt, K. Hagel, F. Haddad, A. Kolomiets, Y. Lou, J. Li, M. Shimooka, S. Shlomo, D. Utley, B. Xiao, N. Mdeiwayeh, J. B. Natowitz, Z. Majka, J. Cibor, T. Kozik, and Z. Sosin, Phys. Rev. C **55**, 227 (1997).
- [15] K. Kwiatkowski, A. S. Botvina, D. S. Bracken, E. R. Foxford, W. A. Friedman, R. G. Korteling, K. B. Morley, E. C. Pollacco, V. E. Viola and C. Volant, Phys. Lett. **B423**, 21 (1998).
- [16] K. B. Morley, K. Kwiatkowski, D. S. Bracken, E. Renshaw Foxford, V. E. Viola, L. W. Woo, N. R. Yoder, R. Legrain, E. C. Pollacco, C. Volant, R. G. Korteling, H. Breuer and J. Brzychczyk, Phys. Rev. C **54**, 737 (1996); *Ibid*, **54**, 749 (1996).
- [17] J. Cibor, R. Wada, K. Hagel, M. Lunardon, N. Marie, R. Alfaro, W. Q. Shen, B. Xiao Y. Zhao, J. Li, B. A. Li, M. Murray, J. B. Natowitz, Z. Majka and P. Staszal, Phys. Lett. **B473**, 29 (2000).
- [18] K Hagel, R. Wada, J. Cibor, M. Lunardon, N. Marie, R. Alfaro, W. Shen, B. Xiao, Y. Zhao, Z. Majka, J. Li, P. Staszal, B-A Li, M. Murray, T. Keutgen, A. Bonasera and J. B. Natowitz, Phys. Rev. C **62**, 034607-1 (2000).
- [19] A. Ruangma et al, the IsiS Collaboration, nucl-ex/0110004, Submitted to Phys. Rev. C, (2001).
- [20] B. Borderie, nucl-ex/0102016, LANL preprint server, Invited talk to Bologna 2000, Structure of the Nucleus at the Dawn of the Century, Bologna, Italy, May 29 - June 3 2000, to be published by World Scientific.
- [21] S. Das Gupta, A. Z. Mekjian, M. B. Tsang nucl-th/0009033, LANL preprint server, submitted to Adv. Nucl. Phys. (2001).
- [22] J. B. Elliott, L. G. Moretto, L. Phair, G. J. Wozniak, T. Lefort, L. Beaulieu, K. Kwiatkowski, W. C. Hsi, L. Pienkowski, H. Breuer, R. G. Korteling, R. Laforest, E. Martin, E. Ramakrishnan, D. Rowland, A. Ruangma, V. E. Viola, E. Winchester, S. J. Yennello nucl-ex/0104013, LANL preprint server, submitted to Phys. Rev. Lett (2001).
- [23] S. Albergo, S. Costa, E. Costanzo and A. Rubbino, Nuovo Cimento A **89**, 1 (1985).
- [24] M. B. Tsang, W. G. Lynch, H. Xi, and W. A. Friedman, Phys. Rev. Lett. **78**, 3836 (1997).
- [25] T. Lefort, K. Kwiatkowski, W.C. Hsi, L. Pienkowski, L. Beaulieu, B. Back, H. Breuer, S. Gushue, R. G. Korteling, R. Laforest, E. Martin, E. Ramakrishnan, L. P. Remsberg, D. Rowland, A. Ruangma, V. E. Viola, E. Winchester, and S. J. Yennello, Phys. Rev. Lett. **83**, 4033 (1999).
- [26] F. Goldenbaum, W. Bohne, J. Eades, T. v. Egidy, P. Figuera, H. Fuchs, J. Galin, Ye. S. Golubeva, K. Gulda D. Hilscher, A. S. Iljinov, U. Jahnke, J. Jastrzebski, W. Kurcewicz, B. Lott, M. Morjean, G. Pausch, A. Pghaire, L. Pienkowski, D. Polster, S. Proschitzki, B. Quednau, H.Rossner, S. Schmid, W. Schmid, and P. Ziem, Phys. Rev. Lett. **77**, 1230 (1996).
- [27] Y. G. Ma, A. Siwek, J. Peter, F. Gulminelli, R. Dayras, L. Nalpas, B. Tamain, E. Vient, G. Auger, C. O. Bacri, J. F. Benlliure, E. Bisquer, B. Borderie, R. Bougault, R. Brou, J.L. Charvet, A. Chbihi, J. Colin, D. Cussol, E. De-Filippo, A. Demeyer, D. Dore, D. Durand, P. Ecomard, P. Eudes, E. Gerlic, D. Gourio, D. Guinet, R. Laforest, P. Lautesse, J. . Laville, L. Lebreton, J. . Lecolley, A. LeFevre, T. Lefort, R. Legrain, O. Lopez, M. Louvel, J. Lukasik, N. Marie, V. Metivier, A. Ouatizerga, M. Parlog, E. Plagnol, A. Rahmani, T. Reposeur, M. F. Rivet, E. Rosato, E. SaintLaurent, M. Squalli, J. C. Steckmeyer, M. Stern, L. TassanGot, C. Volant and J. P. Wieleczko, Phys. Lett. **B390**, 41 (1997).
- [28] J. Peter, Nuov. Cim. A **111**, 977 (1998).
- [29] J. Peter, F. Gulminelli, Y. G. Ma, A. Siwek, F. Bocage, R. Bougault, R. Brou, J. Colin, D. Cussol, D. Durand, E. Genouin-Duhamel, R. Laforest, J. F. Lecolley, T. Lefort, O. Lopez, M. Louvel, V. Metivier, N. Le Neindre, A.D. Nguyen, J. C. Steckmeyer, B. Tamain, E. Vient, M. Assenard, P. Eudes, M. Germain, D. Gourio, J. L. Laville and T. Reposeur Rev. Mex. Fis. **44**, 97 (1998).
- [30] D. Dore, P. Buchet, J. L. Charvet, R. Dayras, L. Nalpas, D. Cussol, T. Lefort, R. Legrain, C. Volant, G. Auger, C. O. Bacri, N. Bellaize, F. Bocage, R. Bougault, B. Bouriquet, R. Brou, A. Chbihi, J. Colin, A. Demeyer, D. Durand, J. D. Frankland, E. Galichet, E. Genouin-Duhamel, E. Gerlic, D. Guinet, S. Hudan, P. Lautesse, F. Lavaud, J. L. Laville, J. F. Lecolley, C. Leduc, N. Le Neindre, O. Lopez, M. Louvel, A. M. Maskay, J. Normand, M. Parlog, P. Pawlowski, E. Plagnol, M. F. Rivet, E. Rosato, F. Saint-Laurent, J. C. Steckmeyer, M. Stern, G. Tabacaru, B. Tamain, L. Tassan-Got, O. Tirel, E. Vient, J. P. Wieleczko, Phys. Lett. B **491**, 15 (2000).
- [31] J. B. Natowitz, K. Hagel, R. Wada, Z. Majka, P. Gonthier, J. Li, N. Mdeiwayeh, B. Xiao, and Y. Zhao, Phys. Rev. C **52**, R2322 (1995).
- [32] R. Hasse and P. Schuck, Phys. Lett. **B179**, 313 (1986).
- [33] S. Shlomo and J. B. Natowitz, Phys. Lett. **B252**, 187 (1990).
- [34] S. Shlomo and J. B. Natowitz, Phys. Rev. C **44**, 2878 (1991).
- [35] J. B. Natowitz, D. Fabris, F. Haddad, K. Hagel, J. Li, Y. Lou, N. Mdeiwayeh, G. Nebbia, G. Prete, R. Tezkratt, D. Utley, G. Viesti, R. Wada and B. Xiao. Proceedings of the Nuclear Chemistry Award Symposium, 209th Meeting of the American Chemical Society, Anaheim, World Scientific Press, Singapore, (1995 ) P1.
- [36] A. Bonasera, M. Bruno, C. O. Dorso and P.F. Mastinu,

- Riv. Del Nuov. Cim. **23**, 1 (2000).
- [37] A. Strachan and C. O. Dorso, Phys. Rev. C **58**, R632 (1998).
- [38] Y. Sugawa and H. Horiuchi, Phys. Rev. C **60**, 607 (1999).
- [39] H. Feldmeier and J. Schnack Rev. Mod. Phys. **72**, 655 (2000).
- [40] J. N. De, S. Das Gupta, S. Shlomo, and S. K. Samaddar, Phys. Rev. C **55**, R1641 (1997).
- [41] V. M. Kolomietz, A.I. Sanzhur, S. Shlomo and S.A. Firin, Phys. Rev. C **64**, 024315 (2001).
- [42] H. Jaqaman, A. Z. Mekjian, and L. Zamick, Phys. Rev. C **27**, 2782 (1983).
- [43] H. Q. Song and R. K. Su, Phys. Rev. C **44**, 2505 (1991).
- [44] J. Besprovaný and S. Levitt Phys. Lett. **B217**,1 (1989)
- [45] S.Levit and P.Bonche, Nucl. Phys. **A437**, 426 (1985).
- [45] Y. Zhang, R. Su, H. Song, and F. Lin, Phys. Rev. C **54**, 1137 (1996).
- [46] L. L. Zhang, H. Q. Song, P. Wang, and R. K. Su, Phys. Rev. C **59**, 3292 (1999).
- [47] R. J. Furnstahl, H. B. Tang, and B. D. Serot, Phys. Rev. C **52**, 1368 (1995).
- [48] D. H. Youngblood, H. L. Clark and Y. W. Lui, Nucl. Phys. **A649**, 49C (1999).
- [49] A. L. Goodman, J. I. Kapusta, and A. Z. Mekjian, Phys. Rev. C **30**, 851(1984).
- [50] J. B. Elliott, S. Albergo, F. Bieser, F. P. Brady, Z. Caccia, D. A. Cebr, A. D. Chacon, J. L. Chance, Y. Choi, S. Costa, M. L. Gilkes, J. A. Hauger, A. S. Hirsch, E. L. Hjort, A. Insolia, M. Justice, D. Keane, J. C. Kintner, V. Lindenstruth, M. A. Lisa, H. S. Matis, M. McMahan, C. McParland, W. F. J. Mller, D. L. Olson, M. D. Partlan, N. T. Porile, R. Potenza, G. Rai, J. Rasmussen, H. G. Ritter, J. Romanski, J. L. Romero, G. V. Russo, H. Sann, R. P. Scharenberg, A. Scott, Y. Shao, B. K. Srivastava, T. J. M. Symons, M. Tincknell, C. Tuv, S. Wang, P. G. Warren, H. H. Wieman, T. Wienold, and K. Wolf, Phys. Rev. C **62**, 064603 (2000) and references therein.
- [51] C. M. Mader, A. Chappars, J. B. Elliott, L. G. Moretto, L. Phair, G. J. Wozniak, nucl-th/0103030, LANL preprint server (2001).
- [52] P. Chomaz and F. Gulminelli, Phys. Lett. **B447**, 221 (1999).
- [53] U. Heinz hep-ph/0009170, LANL preprint server, Proceedings of the 7th International Conference on Nucleus-Nucleus Collisions (NN2000), Strasbourg, 3-7 July 2000, Nucl. Phys. **A685**, 414c (2000).
- [54] H. Müller and B. D. Serot, Phys. Rev. C **52**, 2072 (1995).
- [55] B. K. Srivastava et al., nucl-ex/0107018
- [56] C. O. Dorso and A. Bonasera, Eur. Phys. J. **11** 421 (2001).

TABLE I: Summary of Measurements Included in Analysis

Reference	Reactions	Temperature		Excitation Energy	
		Method	Correction	Method	Correction
6	Hagel <i>et al.</i> 19,35 MeV/A N+Sm	He Slope	Cascade Correction	Momentum Transfer	None
7	Wada <i>et al.</i> 30Mev/A O,S+Ag	He Slope	Cascade Correction	Momentum Transfer	None
8	Cussol <i>et al.</i> 36-65Mev/A Ar+Al	He Slope	Cascade Correction	Momentum Transfer	None
9	Chulick <i>et al.</i> 10Mev/A C+Sn	He Slope	None	Momentum Transfer	None
10	Gonin <i>et al.</i> 11Mev/A Ni+Mo	H,He Slope	Subtraction	Calorimetry	None
11	Pochadzalla	1000Mev/A Au+Au	HeLi Isotope Ratio	QSM Model	Calorimetry SMM
12	<i>et al.</i> Odeh				Backtrace
13	Hauger <i>et al.</i> 1A GeV Kr, La, Au+C	HHe Isotope Ratio	SMM Model	Calorimetry	Pre-Eq. Removed
14	Wada <i>et al.</i> 35Mev/A Cu+Au	HHe Isotope Ratio	QSM Model	Calorimetry	Pre-Eq. Removed
15,16	Kwiatkowski <i>et al.</i> 4.8 GeV He+Ag,Au	HHe Isotope Ratio	SMM E Window Correction	Calorimetry	Pre-Eq. Removed
17,18	Cibor <i>et al.</i> 47Mev/A C, Ne, Ar, Zn Hagel <i>et al.</i> + Med. Mass and Au	HHe Isotope Ratio	None	Calorimetry	Pre-Eq. Removed
19	Ruangma <i>et al.</i> 8 GeV/c pion+Au	HHe Isotope Ratio	Tsang Systematics	Calorimetry	Pre-Eq. Removed

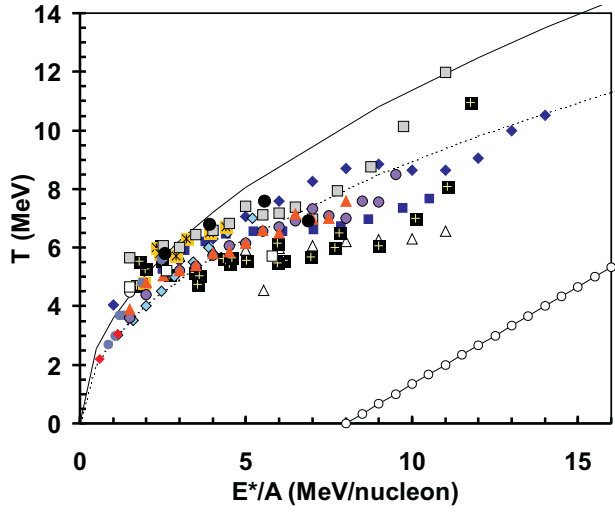


FIG. 1: Caloric curve data from references [6, 7, 8, 9, 10, 11, 12, 13, 14, 15, 16, 17, 18, 19] Measurements of temperature vs excitation energy per nucleon are represented by symbols. Reference [6]-dark gray filled circles; Reference [7] -filled gray squares with black stars; Reference [8] - filled light-gray diamonds; Reference [9] - filled dark-gray diamonds; Reference [10] - open circles; References [11, 12] - black filled squares with white plus signs; Reference [13] - black diamonds ( $^{84}\text{Kr}$ ), black squares ( $^{134}\text{La}$ ) and open triangles( $^{197}\text{Au}$ ); Reference [14] - Black triangles; References [15, 16] - light-gray filled circles (Ag); light-gray filled triangles ( $^{197}\text{Au}$ ); References [17, 18] - black filled circles; Reference [19] - Light- gray filled squares. Fermi-gas model lines for  $K=8$  (dashed line) and  $K=13$  (solid line) and a “total vaporization” line (see text) - connected small open circles are shown for comparison.

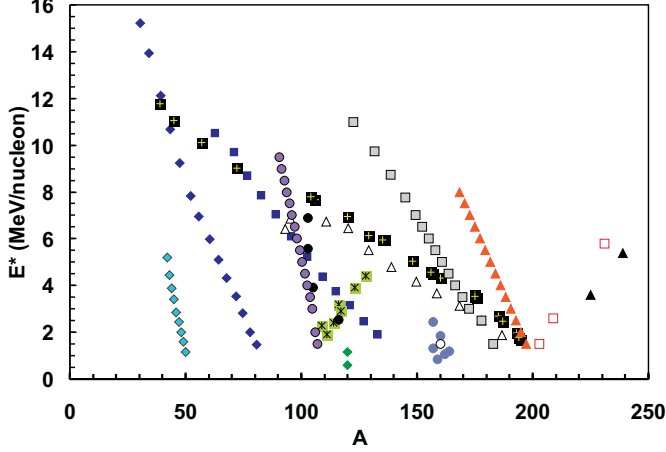


FIG. 2: Excitation Energy per nucleon as a function of  $A$ . Reference [6]-dark gray filled circles; Reference [7] -filled gray squares with black stars; Reference [8] - filled light-gray diamonds; Reference [9] - filled dark-gray diamonds; Reference [10] - open circles; References [11, 12] - black filled squares with white plus signs; Reference [13] - black diamonds ( $^{84}\text{Kr}$ ), black squares ( $^{134}\text{La}$ ) and open triangles( $^{197}\text{Au}$ ); Reference [14] - Black triangles; References [15, 16] - light-gray filled circles (Ag); light-gray filled triangles ( $^{197}\text{Au}$ ); References [17, 18] - black filled circles; Reference [19] - Light- gray filled squares.

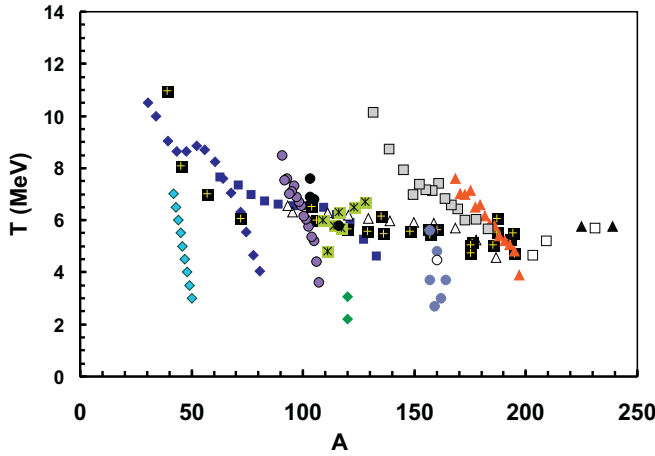


FIG. 3: Temperature as a function of  $A$ , the mass number of the primary de-exciting nucleus. Reference [6]-dark gray filled circles; Reference [7] -filled gray squares with black stars; Reference [8] - filled light-gray diamonds; Reference [9] - filled dark-gray diamonds; Reference [10] - open circles; References [11, 12] - black filled squares with white plus signs; Reference [13] - black diamonds ( $^{84}\text{Kr}$ ), black squares ( $^{134}\text{La}$ ) and open triangles( $^{197}\text{Au}$ ); Reference [14] - Black triangles; References [15, 16] - light-gray filled circles (Ag); light-gray filled triangles ( $^{197}\text{Au}$ ); References [17, 18] - black filled circles; Reference [19] - Light- gray filled squares.

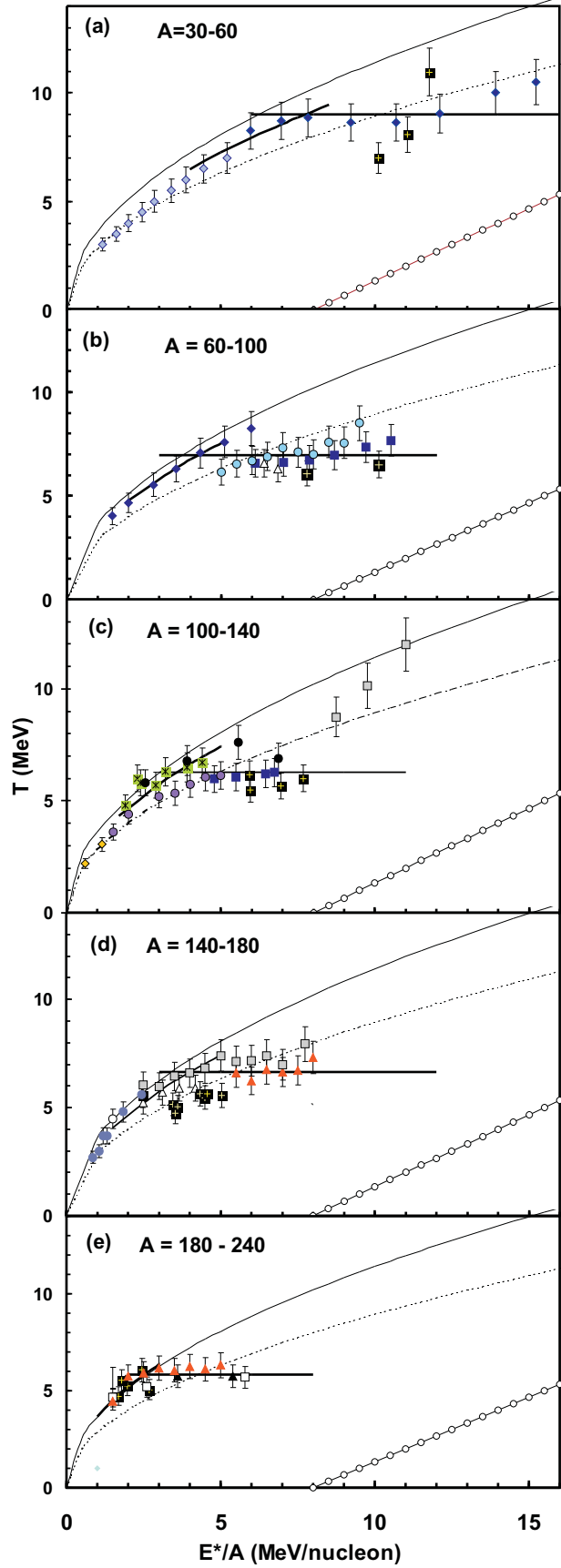


FIG. 4: Caloric curves for five selected regions of mass. Reference [6]-dark gray filled circles; Reference [7]-filled gray squares with black stars; Reference [8]-filled light-gray dia-

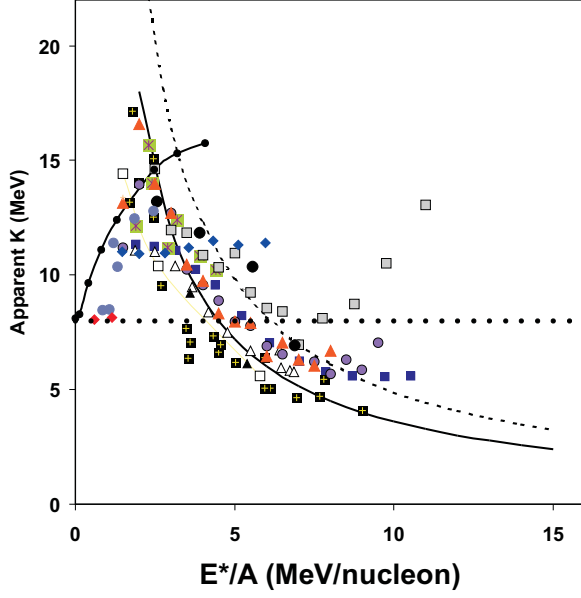


FIG. 5: Apparent Fermi gas level density parameters as a function of excitation energy. Data are from references in Table I. Data for nuclei with  $A < 60$  are not included. (See text.) The horizontal dotted line represents a constant value of  $K=8$ . The solid line with solid dots represents the theoretical prediction of reference [34]. Two additional lines are shown, representing the values of  $K$  corresponding to a constant  $T=6$  MeV (solid line) and  $T=7$  MeV (dashed line). Reference [6]-dark gray filled circles; Reference [7]-filled gray squares with black stars; Reference [8]-filled light-gray diamonds; Reference [9]-filled dark-gray diamonds; Reference [10]-open circles; References [11, 12]-black filled squares with white plus signs; Reference [13]-black diamonds ( $^{84}\text{Kr}$ ), black squares ( $^{134}\text{La}$ ) and open triangles ( $^{197}\text{Au}$ ); Reference [14]-Black triangles; References [15, 16]-light-gray filled circles (Ag); light-gray filled triangles ( $^{197}\text{Au}$ ); References [17, 18]-black filled circles; Reference [19]-Light-gray filled squares.

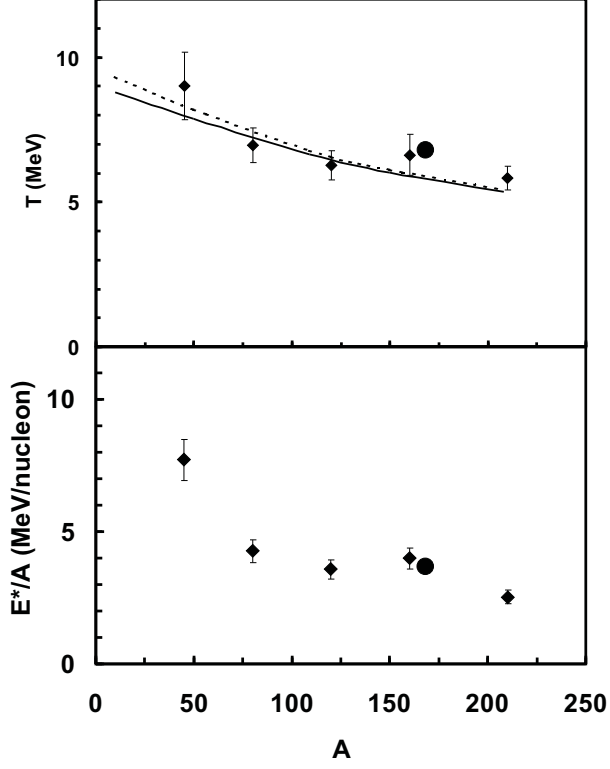


FIG. 6: Limiting values of  $T$  (a) and  $E^*/A$  at which  $T_{limit}$  is reached (b) are indicated by solid diamonds. The critical temperature and excitation energy derived from the Fisher droplet model analysis of Elliott et al. [22] are represented by solid circles. The lines in the top panel represent the calculated Coulomb instability temperatures from references [45] (dashed line) and [46] (solid line).